Am J Physiol Cell Physiol 292: C778–C787, 2007.
First published September 6, 2006; doi:10.1152/ajpcell.00259.2006.

Episodic ataxia type 1 mutation F184C alters Zn^{2+}-induced modulation of the human K^+ channel Kv1.4-Kv1.1/Kvβ1.1

Paola Imbrici, Maria Cristina D'Adamo, Antonella Cusimano, and Mauro Pessia

Section of Human Physiology, Department of Internal Medicine, University of Perugia School of Medicine, Perugia, Italy

Submitted 11 May 2006; accepted in final form 28 July 2006

Imbrici P, D'Adamo MC, Cusimano A, Pessia M. Episodic ataxia type 1 mutation F184C alters Zn^{2+}-induced modulation of the human K^+ channel Kv1.4-Kv1.1/Kvβ1.1. *Am J Physiol Cell Physiol* 292: C778–C787, 2007. First published September 6, 2006; doi:10.1152/ajpcell.00259.2006.—Episodic ataxia type 1 (EA1) is a *Shaker*-like channelopathy characterized by continuous myokymia and attacks of imbalance with jerking movements of the head, arms, and legs. Although altered expression and gating properties of Kv1.1 channels underlie EA1, several disease-causing mechanisms remain poorly understood. It is likely that Kv1.1, Kv1.4, and Kvβ1.1 subunits form heteromeric channels at hippocampal mossy fiber boutons from which Zn^{2+} ions are released into the synaptic cleft in a Ca^{2+}-dependent fashion. The sensitivity of this macromolecular channel complex to Zn^{2+} is unknown. Here, we show that this heteromeric channel possesses a high-affinity (<10 μM) and a low-affinity (<0.5 mM) site for Zn^{2+}, which are likely to regulate channel availability at distinct presynaptic membranes. Furthermore, the EA1 mutation F184C, located within the S1 segment of the Kv1.1 subunit, markedly decreased the equilibrium dissociation constants for Zn^{2+} binding to the high- and low-affinity sites. The functional characterization of the Zn^{2+} effects on heteromeric channels harboring the F184C mutation also showed that this ion significantly *1*) slowed the activation rate of the channel, *2*) increased the time to reach peak current amplitude, *3*) decreased the rate and amount of current undergoing N-type inactivation, and *4*) slowed the repriming of the channel compared with wild-type channels. These results demonstrate that the EA1 mutation F184C will not only sensitize the homomeric Kv1.1 channel to extracellular Zn^{2+}, but it will also endow heteromeric channels with a higher sensitivity to this metal ion. During the vesicular release of Zn^{2+}, its effects will be in addition to the intrinsic gating defects caused by the mutation, which is likely to exacerbate the symptoms by impairing the integration and transmission of signals within specific brain areas.

shaker channel gating; episodic ataxia type 1; Xenopus laevis cocytes

EPISODIC ATAXIA type 1 (EA1) is an autosomal dominant neurological disorder affecting central and peripheral nerve functions. The disease is characterized by symptomatic attacks of imbalance and uncontrolled movements that may be triggered by physical or emotional stress (3, 8, 12, 22, 60). The duration of the attacks of ataxia varies: they may occur several times a day or once a year. Although the symptoms vary between and within families, two symptoms are always observed: an ataxic gait during attacks and myokymia. The latter symptom is characterized by continuous muscle activity that can be detected as a rhythmic electromyography activity with a pattern of repeated duplets and multiplets (12, 22). Genetic linkage studies have localized the EA1 locus to chromosome 12p13 (36). Subsequently, the *KCNA1* gene, which encodes for the delayed-rectifier K^+ channel Kv1.1, has been identified as underlying EA1 (11). All affected individuals possess heterozygous point mutations at positions highly conserved among the voltage-dependent K^+ channel superfamily (10, 11). Dominant-negative effects or haploinsufficiency may underlie altered K^+ channel function in EA1-affected individuals (65). Most EA1 channels are functional and, depending on the location within the Kv1.1 subunit, produce homomeric channels with biophysical properties that differ from those of wild-type channels (7, 9, 15, 16, 19, 31, 55, 66, 70). Although several lines of evidence indicate that defective delayed rectifier channels underlie EA1, many molecular mechanisms have not been thoroughly characterized (33). Recently, a mouse model of EA1 has been generated by introduction of the V408A mutation into the mouse *Kv1.1* gene. These animals showed impaired motor performance and altered cerebellar GABAergic transmission from the basket cells to the Purkinje cells (27).

When EA1 subunits coassemble with wild-type subunits or with subunits belonging to the same K^+ channel subfamily (e.g., Kv1.2), the resulting heteromeric proteins are endowed with partial EA1 phenotypes (16, 46). Individuals carrying the F184C mutation showed generalized motor seizures, in addition to typical EA1 symptoms (11, 60). This phenylalanine-to-cysteine substitution is located at the COOH-terminal portion of the first transmembrane domain (S1) of the Kv1.1 subunit. In previous studies, we and others showed that the F184C mutation shifted the half-maximal activation voltage ($V_{1/2}$) of Kv1.1 homomeric channels ~25 mV to more depolarized potentials, and slowed the time constants of activation by nearly twofold (1, 9, 14, 65). Recently, we also showed that this mutation sensitizes homomeric Kv1.1 channels to extracellular Zn^{2+} (14). However, we did not investigate whether this mutation also affects the Zn^{2+} sensitivity of channels composed of Kv1.4, Kv1.1, and Kvβ1.1 subunits, inasmuch as these subunits are likely to form a macromolecular channel complex in several brain structures in which Zn^{2+} plays a role (24, 44, 48, 50, 51, 59, 62).

Specific neurons are able to store Zn^{2+} within vesicles. Their release into the synaptic cleft is regulated by the frequency and intensity of the stimuli by means of Ca^{2+}-dependent mechanisms. Neuron excitability is affected by Zn^{2+}, which modulates the activity of selected members of ligand- and voltage-gated ion channels (for reviews see Refs. 20, 25, 40, 54, 56, 57). The location of this ion and its release pattern have been established across the brain by use of Zn^{2+} fluoro-

Address for reprint requests and other correspondence: M. Pessia, Section of Human Physiology, Dept. of Internal Medicine, Univ. of Perugia School of Medicine, Via del Giochetto, I-06126 Perugia, Italy (e-mail: pessia@unipg.it).

The costs of publication of this article were defrayed in part by the payment of page charges. The article must therefore be hereby marked "*advertisement*" in accordance with 18 U.S.C. Section 1734 solely to indicate this fact.

phores, radiolabeled Zn^{2+}, and selective chelators (20, 21, 30, 35, 58, 63). In particular, Zn^{2+} is released from mossy fiber terminals in the hippocampus (4, 61, 64). A growing body of evidence indicates that Kv1.1, Kv1.4, and, Kvβ1.1 subunits form heteromeric channels at hippocampal mossy fiber boutons (44, 48, 49, 51, 53, 59). Moreover, patch-clamp recordings from such presynaptic terminals suggest that this macromolecular channel complex regulates the activity-dependent spike broadening of hippocampal mossy fiber boutons and, as a consequence, the amount of neurotransmitter released during high-frequency stimuli (23). Thus an altered Zn^{2+}-mediated modulation of heteromeric channel activity may exert a remarkable impact on the hippocampal integration and transmission of signals.

Here we show that the EA1 mutation F184C will not only sensitize the homomeric Kv1.1 channel to extracellular Zn^{2+}, but it will also endow heteromeric channels, composed of human Kv1.1, Kv1.4, and Kvβ1.1 subunits, with a higher sensitivity to Zn^{2+}, which also significantly modifies several biophysical properties of the mutated channel.

METHODS

Molecular biology. The human β-subunits were kindly provided by Prof. Olaf Pongs (Institut für Neurale Signalverarbeitung, Center for Molecular Neurobiology Hamburg, Universität Hamburg, Hamburg, Germany), and the human Kv1.4 subunit was cloned in our laboratory. To study the activity of channels composed of two human Kv1.1 and two human Kv1.4 subunits, the relevant cDNAs were linked as dimers (15). To concatenate the human Kv1.4 wild-type subunits with the episodic ataxia human Kv1.1 subunits as dimers, the stop codon of the first subunit was removed and a linker encoding 10 glutamine residues was inserted between the last codon of the 5′-subunit coding sequence and the initiator codon of the following subunit. This was achieved using a sequential PCR protocol similar to that used by Horton et al. (29). Briefly, junctions were generated by overlap extension of the PCR primers that also encoded the glutamine linker. The dimers were constructed in pGEMA, a modified version of pGEM9zf (Promega), with a stretch of 40 A-T base pairs inserted just upstream of the Tth111I site. The QuikChange Site-Directed Mutagenesis kit (Stratagene) was used according to the manufacturer's instructions to introduce the F184C mutation into the human Kv1.1 subunit cDNA. The nucleotide sequences of all linked subunits and throughout the joined segments were determined by automated sequencing. Oligonucleotides were obtained from EUROBIO (Milan, Italy). All channel subunits were subcloned into the oocyte's expression vector pBF, which provides 5′- and 3′-untranslated regions from the *Xenopus* β-globin gene flanking a polylinker containing multiple restriction sites. Capped mRNAs were synthesized in vitro using the SP6 mMESSAGE mMACHINE kit (Ambion).

Oocyte preparation and RNA injection. Procedures involving *Xenopus laevis* and their care were conducted in conformity with institutional guidelines, which are in compliance with national (D.L. no. 116, G.U., Suppl. 40, 18 February 1992) and international [EEC Council Directive 86/609, OJ L 358,1, 12 December 1987; National Institutes of Health *Guide for the Care and Use of Laboratory Animals* (NIH Publ. No. 85-23, 1985); and "Guidelines for the Use of Animals in Biomedical Research" (*Thromb Haemost* 58: 1078–1084, 1987)] laws and policies.

The animals underwent no more than two surgical operations, with an interval of ≥3 wk between the procedures. *X. laevis* were anesthetized with an aerated solution containing 5 mM 3-aminobenzoic acid ethyl ester methansulfonate salt and 60 mM sodium bicarbonate (pH 7.3). The ovary was dissected, and the oocytes were digested in OR-2 solution containing collagenase A (Sigma; 0.5 U/ml). Stage V–VI oocytes were isolated and stored at 16°C in fresh ND96 medium (96 mM NaCl, 2 mM KCl, 1 mM $MgCl_2$, 1.8 mM $CaCl_2$, 5 mM HEPES, and 50 μg/ml gentamicin).

After 24 h, a nanoliter injector (WPI, Nanoject, Drummond, Broomall, PA) was used to microinject in vitro transcribed mRNAs into the oocytes, which were then incubated at 16°C. Typically, every oocyte was injected with 50 nl of a solution containing the relevant mRNA. The amount of mRNAs was quantified using a spectrophotometer and by ethidium bromide staining. Human Kvα1.4-1.1 and human Kvβ1 mRNAs were injected into the oocytes in a ratio of 1:20–1:40.

Electrophysiology. Electrophysiological recordings and data analysis were performed as previously described (14, 15). Briefly, two-electrode voltage-clamp recordings were obtained from *Xenopus* oocytes at ~22°C 1–8 days after injection. An amplifier (GeneClamp 500, Axon Instruments) interfaced to a personal computer with an ITC-16 interface (Instrutech) was used. Microelectrodes were filled with 3 M KCl; resistance of the microelectrodes was 0.1–0.5 MΩ. The recording solution contained (in mM) 96 NaCl, 2 KCl, 1 $MgCl_2$, 1.8 $CaCl_2$, and 5 HEPES (pH 7.4). Currents were evoked by voltage commands from a holding potential of −80 mV. The recordings were filtered at 2 kHz and acquired at 5 kHz with Pulse software (HEKA Elektronik). Data analysis was performed using IGOR (Wavemetrics), PulseFit (HEKA Elektronik), and KaleidaGraph (Synergy Software) software. Leak and capacitative currents were subtracted using a P/4 protocol. An unpaired Student's test was used to determine the statistical significance. $P < 0.05$ was considered significant.

RESULTS

Functional expression of wild-type and F184C channels composed of Kv1.1, Kv1.4, and Kvβ1.1 subunits. To investigate the effects of the F184C mutation on the biophysical properties of heteromeric channels and to assess their sensitivity to extracellular Zn^{2+}, the human Kv1.4 subunit was concatenated with the Kv1.1 wild-type or Kv1.1F184C, as dimers, by means of a flexible glutamine linker. Two constructs were generated: Kv1.4-1.1 wild-type (WT) and Kv1.4-1.1F184C (F184C). The expression of these concatemers in *Xenopus* oocytes gave rise to functional delayed-rectifier currents, presumably arising from a homogeneous population of heterotetrameric channels composed of two subunits of each type. Figure 1*A* shows a representative current family recorded in two-electrode voltage-clamp configuration from a cell expressing WT channels. These currents were characterized by rapid N-type inactivation conferred by the Kv1.4 subunit, which possesses an inactivation particle at its NH_2 terminus (Fig. 1, *A* and *inset*) (39, 43, 50). The dimeric channel was also coexpressed with the auxiliary subunit Kvβ1.1. As expected, the current family recorded from these cells showed that the human Kvβ1.1 subunit further accelerated the inactivation of the channel by providing four additional inactivation particles (Fig. 1, *B* and *inset*) (26, 38, 39, 47, 69). The current traces recorded from cells expressing the F184C channels showed altered kinetics of activation and inactivation in the presence and absence of Kvβ1.1 subunits (Fig. 1, *C* and *D*; see below).

F184C mutation increases Zn^{2+}-induced inhibition of heteromeric channels. To determine the Zn^{2+} sensitivity of WT and F184C channels with or without Kvβ1.1 subunits, macroscopic currents were recorded before and during the superfusion of a solution containing $ZnCl_2$ at several concentrations into the recording chamber. The concentration-response curves for Zn^{2+}-induced inhibition were calculated at 0 and +60 mV (Fig. 2). However, the open probabilities of WT and F184C

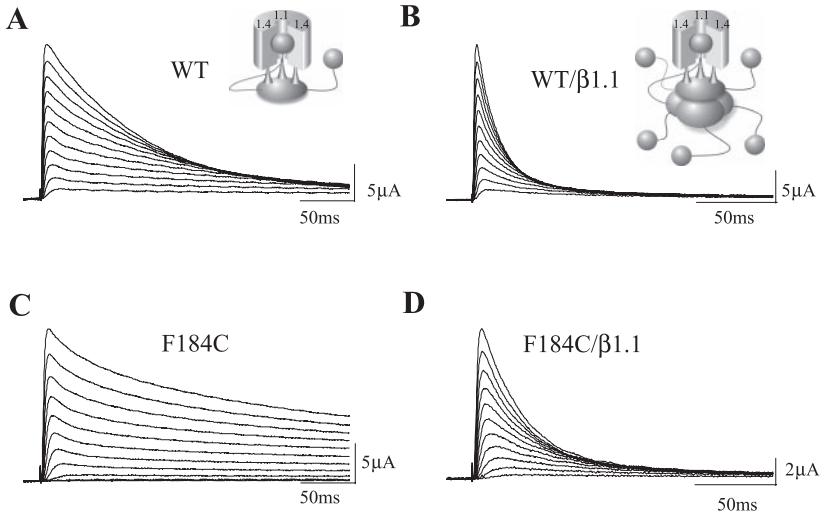

Fig. 1. Heterologous expression of wild-type (WT) and F184C heterodimeric channels with and without the auxiliary subunit Kvβ1.1. Representative current traces were recorded from *Xenopus* oocytes injected with Kv1.4-1.1WT (*A*; WT), Kv1.4-1.1WT + Kvβ1.1 (*B*; WT/β1.1), Kv1.4-1.1F184C (*C*; F184C), and Kv1.4-Kv1.1F184C + Kvβ1.1 (*D*; F184C/β1.1) mRNA. Membrane potential was held at −80 mV, and current families were evoked by depolarizing pulses from −20 to +60 mV. *Insets*: main molecular features of Kv1.4-1.1 (*left*) and Kv1.4-Kv1.1 + Kvβ1.1 (*right*) constructs. Foreground Kv1.1 subunit has been removed for clarity.

channels, with or without Kvβ1.1 subunits, are maximal at +60 mV before and after the application of Zn^{2+}, which shifted the $V_{1/2}$ of channel activation only 3–10 mV to more depolarized potentials (not shown). This test potential also corresponds approximately to the peak of the action potential, and it allows us to obtain pathophysiologically relevant information. The Zn^{2+} concentration/inhibition data points for WT channels were best fitted by the sum of two Hill equations in the presence or absence of Kvβ1.1 subunits (Fig. 2). These results revealed, first, that heteromeric channels composed of Kv1.4-1.1 or Kv1.4-1.1/Kvβ1.1 subunits possess a high- and a low-affinity binding site for Zn^{2+}. The low- and high-affinity equilibrium dissociation constants for Zn^{2+} binding (K_{Zn}) were calculated at 0 and 60 mV (Table 1). Unexpectedly, we observed that the auxiliary Kvβ1.1 subunits increased the sensitivity of WT channels to Zn^{2+}-induced inhibition by decreasing the low-affinity K_{Zn} ~2.7- and ~3.8-fold at 0 and +60 mV, respectively (Table 1). The concentration-response relations were shifted leftward by the F184C mutation (Fig. 2). Overall, the F184C mutation significantly decreased the K_{Zn} values of the high- and low-affinity binding sites to Zn^{2+}-induced current inhibition of Kv1.4-1.1 and Kv1.4-1.1/Kvβ1.1 channels (Table 1). Moreover, the low- and high-affinity K_{Zn} values of WT and F184C channels were markedly smaller at less depolarized potentials (Table 1) (24). Taken together, these findings imply that Zn^{2+} may regulate the transmission of signals by modulating the availability of heteromeric WT channels at distinct synapses. The availability of F184C channels is further reduced by Zn^{2+} because of their higher sensitivity for this metal ion.

Effects of Zn^{2+} on activation kinetics of F184C channels. Little information is available regarding the dynamics of Zn^{2+} within the synapse. In particular, the mechanisms regulating the patterns of release, the peak concentrations, the rates of removal, and the distance that it disperses from its release site(s) are not well understood. Measurements obtained from imaging or use of chelating agents suggest that the peak concentrations of Zn^{2+} in the synapse may be transiently quite high, quickly dissipating to 10–30 μM (20, 35, 54, 58). Thus we used 10 μM Zn^{2+} for our study, inasmuch as this concentration is likely to be within a physiological range at mossy fiber synapses (61) and is comparable to the high-affinity K_{Zn}

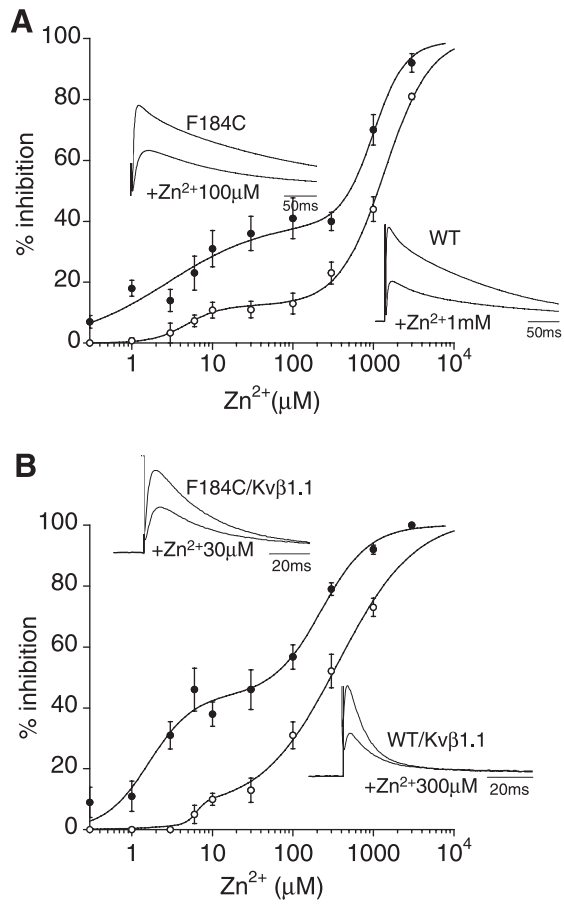

Fig. 2. F184C mutation sensitizes heteromeric channels to extracellular Zn^{2+}. *A*: dose-response curves for WT (○) and F184C (●) channels. *B*: dose-response curves for WT/β1.1 (○) and F184C/β1.1 (●) channels. *Insets*: sample traces for channels recorded before and after superfusion of $ZnCl_2$. Data points were best fitted with the sum of 2 Hill equations: $y = A_1/1 + ([Zn^{2+}]/K_{Zn\,1})^{nH_1} + A_2/1 + ([Zn^{2+}]/K_{Zn\,2})^{nH_2}$, where A_1 and A_2 are relative amplitudes of each component, nH_1 and nH_2 are the Hill coefficients, and $K_{Zn\,1}$ and $K_{Zn\,2}$ are the equilibrium dissociation constants for Zn^{2+} binding to the high- and low-affinity sites, respectively. Solid and dashed lines show fit with the Hill equation before and after application of $ZnCl_2$, respectively. Correlation coefficient (R^2) = 0.99. Values are means ± SE of 6–12 cells.

Table 1. *Apparênt equilibrium dissociation constants for Zn^{2+} binding to low- and high-affinity sites*

	0 mV		+60 mV	
	K_{Zn1}	K_{Zn2}	K_{Zn1}	K_{Zn2}
WT	3.8±1.4 (13)	385±62	4.8±1.1 (12)	1,385±73
F184C	1.35±0.5 (40)	222±54	3.8±0.9 (44)	1,044±160
WT + β1.1	2.3±1.6 (10)	142±7.5	6.4±1.5 (7)	365±35
F184C + β1.1	1.1±0.2 (52)	159±33	1.6±0.6 (44)	222±68

Values are means ± SE in μM (n = 6–10). Values in parentheses are relative amplitudes (A) expressed as percentages. Equilibrium dissociation constants (K_{Zn1}, K_{Zn2}) were calculated at 0 and +60 mV from fit of data points with the sum of 2 Hill equations (KaleidaGraph, Synergy Software). WT, wild type.

determined in vitro from our heteromeric constructs. In a previous study, we showed that the activation kinetics of homomeric F184C channels were markedly slowed by Zn^{2+} (14). To investigate the effects of Zn^{2+} on heteromeric channel activation, current traces were recorded at +60 mV from oocytes expressing WT and F184C channels before and after the superfusion of 10 μM Zn^{2+}. The overlaid traces show that Zn^{2+} slows the kinetics of activation of F184C channels considerably, whereas those of WT channels were little affected by this ion (Fig. 3*A*). To quantify this phenomenon, a single-exponential function was fitted to the activation traces recorded at several test potentials for WT and F184C channels before and after application of 10 μM Zn^{2+}. Plotting the activation time constants as a function of voltage revealed that Zn^{2+} increased the activation time constant of F184C channels nearly twofold at $V_{1/2}$, whereas WT channel activation was much less affected by this ion (Fig. 3*B*, Table 2). The F184C mutation by itself confers slower kinetics of activation to heteromeric than to WT channels (Fig. 3*B, inset*; Table 2). The superimposed traces in Fig. 3*A* also suggest that the mutation itself and Zn^{2+} affect the time necessary to reach maximal channel activation. Thus the time to reach peak current was calculated as the time from zero current to its maximal amplitude and was plotted as a bar graph. This analysis confirms that

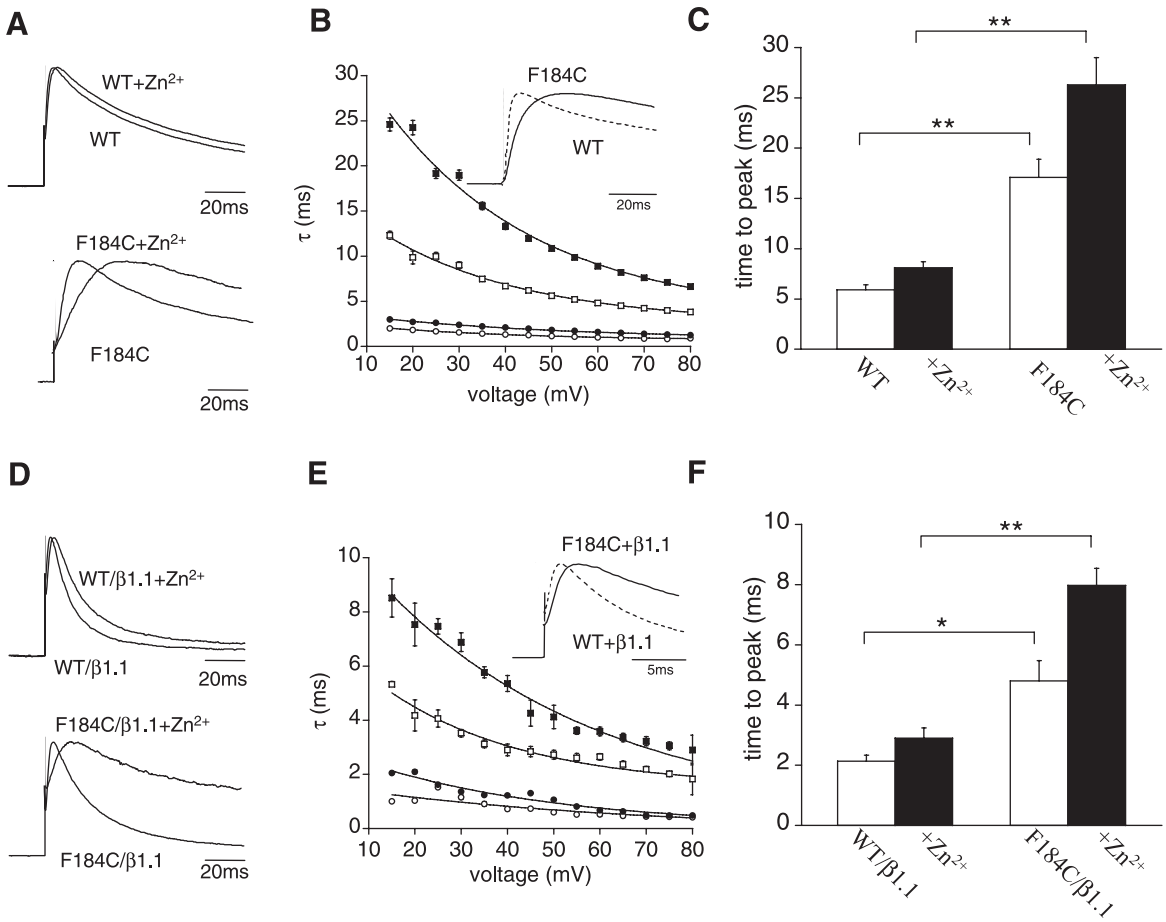

Fig. 3. F184C mutation and Zn^{2+} slow activation kinetics of heteromeric channels. *A*: normalized and superimposed current traces recorded at +60 mV from oocytes before (solid line) and after (dashed line) application of 10 μM Zn^{2+}. *B*: activation time constant (τ) plotted as a function of membrane potential for WT (circles) and Kv1.4-1.1F184C (squares) channels recorded before (open symbols) and after (filled symbols) application of 10 μM Zn^{2+}. Activating current traces, evoked by 10-ms depolarizing pulses from −80 to +80 mV, were fitted with a monoexponential function from which time constants were calculated and plotted as a function of membrane potential. Solid curves show fit with the following equation: $\tau = \tau_{V(1/2)} \exp[(V - V_{1/2})/k]$, where $\tau_{V(1/2)}$ is the time constant at the half-maximal potential ($V_{1/2}$) of each channel type and k is the slope factor for the voltage dependence of the time constants. *C*: time to peak current calculated before and after superfusion of 10 μM Zn^{2+}. *D*: representative current traces recorded from oocytes coexpressing Kvβ1.1 subunits, as described in *A*. *E*: activation time constant plotted as a function of membrane potential for WT/β1.1 (circles) and F184C/β1.1 (squares) channels before (open symbols) and after (filled symbols) superfusion with 10 μM Zn^{2+}. *F*: time to peak current calculated before and after superfusion of 10 μM Zn^{2+}. Values are means ± SE of 6–12 cells. *$P < 0.05$. **$P < 0.001$.

Table 2. *Biophysical parameters for WT and F184C channels expressed alone or with Kvβ1.1 subunits before and after superfusion of 10 μM Zn^{2+}*

Construct	Kinetics of Activation	Kinetics of Inactivation and Recovery From Inactivation		Voltage Dependence of Inactivation	
	$\tau_{activation}$, ms	$\tau_{inactivation}$, ms	$\tau_{recovery}$, s	$V_{1/2}$, mV	k, mV
WT	3.5±0.2	98±8	1.4±0.1	−35.8±0.2	6.0±0.2
F184C	15.5±0.7	143±11	1.9±0.3	−6.8±0.5	14.2±0.4
WT+10 μM Zn^{2+}	4.8±0.1	115±10	2.0±0.3	−42.8±0.2	6.9±0.2
F184C+10 μM Zn^{2+}	31.4±1.1	170±13	2.7±0.6	−7.8±0.5	14.8±0.5
WT+β1.1	3.1±0.3	7.6±0.6 (86)	4.3±0.9	−47.9±0.6	4.8±0.2
F184C+β1.1	4.0±0.7	14.4±2.1 (85)	4.7±1.0	−32.1±0.5	8.6±0.5
WT+β1.1+10 μM Zn^{2+}	4.1±0.4	10.6±0.5 (78)	3.9±0.6	−45.2±0.8	5.3±0.3
F184C+β1.1+10 μM Zn^{2+}	7.0±0.8	26.5±4.3 (84)	7.7±2.1	−31.0±0.8	11.8±0.6

Values are means ± SE; (n = 6); values in parentheses are percentages. $V_{1/2}$, half-maximal potential; k, slope factor; τ, time constant.

the F184C mutation increased the time to maximal channel activation nearly threefold compared with WT channels (Fig. 3*C*). Furthermore, superfusion of 10 μM Zn^{2+} onto oocytes expressing F184C channels significantly increased their time to reach peak current (Fig. 3*C*). The coexpression of Kvβ1.1 subunits apparently accelerated the activation kinetics of WT channels (Fig. 3*E*, Table 2), and, again, the F184C mutation by itself slowed the channel opening kinetics (Fig. 3*E*, Table 2). The application of 10 μM Zn^{2+} markedly increased the time constants of activation (Fig. 3*E*, Table 2) and the time to reach peak current of F184C/Kvβ1.1 channels (Fig. 3*F*, Table 2).

Effects of Zn^{2+} on N-type inactivation and refractory period of F184C channels. The Kv1.4-1.1 channels undergo fast N-type inactivation, which is accelerated by the ancillary subunits Kvβ1.1. Fast inactivation regulates the firing properties of neurons and their response to input stimuli. Thus the effects of the F184C mutation and Zn^{2+} on the biophysical properties of the channel were investigated. Figure 4, *A–D*, shows representative currents, evoked at +60 mV, before and after application of 10 μM Zn^{2+} for WT and F184C channels with or without the coexpression with Kvβ1.1 subunits. These superimposed traces suggest that the F184C mutation by itself and the superfusion of Zn^{2+} changed the amount and the rate of N-type inactivation induced by the Kv1.4 and Kvβ1.1 subunits. The amount of inactivation was then quantified as the ratio of final (at the end of the 1-s depolarizing pulse at +60 mV) to peak current amplitude. The amount of F184C current undergoing inactivation in the presence or absence of auxiliary subunits was significantly decreased compared with the amount of WT current (Fig. 4, *E* and *F*). The application of 10 μM Zn^{2+} reduced these amounts markedly (Fig. 4, *E* and *F*). To determine the inactivation rates, the decaying current traces for WT and F184C channels were fitted with a single-exponential function. The relevant time constants, plotted as a function of voltage, showed that the rate of inactivation was ~1.5-fold slower for F184C than for WT channels at +60 mV (Fig. 4*G*, Table 2). The currents recorded from oocytes coexpressing the Kvβ1.1 subunit were best described with a sum of two exponentials. Again, the F184C mutation slowed the fast component of the time constants nearly twofold, which accounted for 85% of the current (Fig. 1*F*, Table 2). The superfusion of 10 μM Zn^{2+} markedly slowed the N-type inactivation rates of F184C channels in the absence and presence of the Kvβ1.1 subunit (Fig. 4, *G* and *H*, Table 2). By contrast, the effects on WT channels were much less pronounced (Fig. 4, *G* and *H*, Table 2).

To determine the refractory period of all channel types, a double-pulse protocol was used. Two test pulses to +60 mV were delivered for 200 ms from a holding potential of −80 mV and were separated by an interpulse interval of increasing duration. Figure 5, *A* and *C*, shows representative current traces of the recovery from inactivation for WT and F184C channels (alone or coexpressed with Kvβ1.1) before and after the superfusion of 10 μM Zn^{2+} into the recording chamber. To calculate the time constants of the recovery from N-type inactivation, the current amplitudes were normalized, plotted as a function of the interpulse duration, and fitted with a single-exponential function (Fig. 5, *B* and *D*). This analysis revealed that the recovery from inactivation was ~1.4-fold slower for the F184C than for the WT channel (Fig. 5*B*, Table 2). In the presence of the Kvβ1.1 subunit, the recoveries from inactivation for WT and F184C channels were not significantly different (Fig. 5*D*, Table 2). Application of 10 μM Zn^{2+} markedly slowed the recovery of the F184C channel coexpressed with the Kvβ1.1 subunit (Fig. 5*D*, Table 2).

Effects of Zn^{2+} on voltage dependence of F184C channel inactivation. The effects of the F184C mutation on the voltage dependence of heteromeric channel inactivation (steady-state inactivation) were assessed before and after application of 10 μM Zn^{2+}. The amplitude of the outward current was measured during 100-ms depolarizing steps to +60 mV (Fig. 6, *A–C*) after 1-s prepulse potentials from −100 to +60 mV (in 5-mV increments). These currents were normalized, plotted as a function of prepulse potentials, and fitted with the Boltzmann function: $I = 1/\{1 + \exp[(V - V_{1/2})/k]\}$, from which $V_{1/2}$ and the slope factor k were calculated. This analysis showed that the F184C mutation shifted the voltage dependence of the steady-state inactivation of the channel ~29 and ~14 mV with and without Kvβ1.1 subunits, respectively (Fig. 6, *B–D*, Table 2), whereas application of 10 μM Zn^{2+} did not affect the inactivation voltage dependence of WT and F184C channels with or without Kvβ1.1 subunits (Fig. 6, *B–D*, Table 2).

DISCUSSION

In this study, we have demonstrated that distinct heteromeric channels have low- and high-affinity binding sites for Zn^{2+} and that the EA1 mutation F184C endows these channels with a higher sensitivity to Zn^{2+}. Furthermore, we show that the

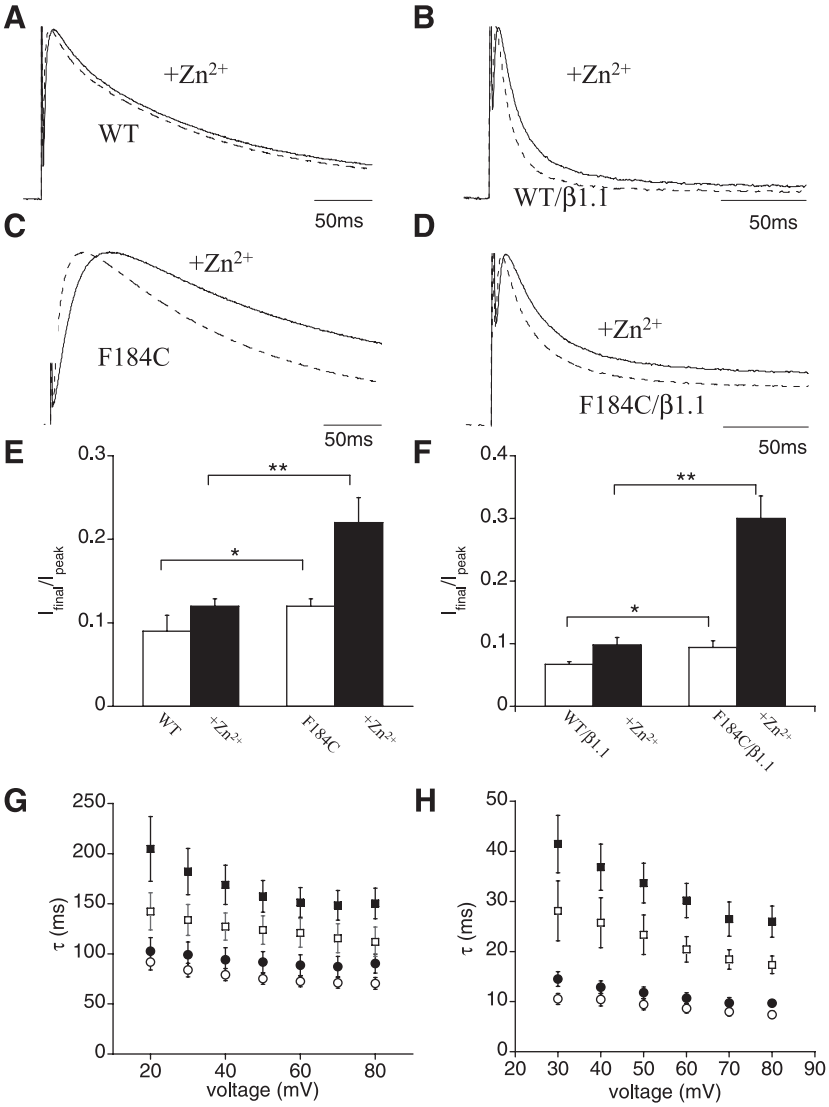

Fig. 4. F184C mutation and Zn^{2+} slow N-type inactivation kinetics of heteromeric channels. *A–D*: superimposed current traces recorded from *Xenopus* oocytes before (dashed line) and after (solid line) superfusion of 10 μM Zn^{2+}. Currents were evoked by depolarizing commands to +60 mV from a holding potential of −80 mV. *E* and *F*: final-to-peak current ratios calculated before and after superfusion of 10 μM Zn^{2+} (1-s depolarizing pulse at +60 mV). *G*: time constants of N-type inactivation plotted as a function of voltage for WT (circles) and F184C (squares) channels calculated before (open symbols) and after (filled symbols) application of 10 μM Zn^{2+}. Decaying current traces were recorded from oocytes expressing WT or F184C channels before and after Zn^{2+} and were best fitted with a single-exponential function from which time constants were calculated. *H*: inactivation time constants plotted as a function of voltage for WT/β1.1 (circles) and F184C/β1.1 (squares) channels calculated before (open symbols) and after (filled symbols) application of 10 μM Zn^{2+}. Decaying current traces for WT/β1.1 and F184C/β1.1 channels were best fitted with a double-exponential function. Fast component, which accounted for 86% of total current, was plotted. Values are means ± SE of 6–12 cells. $*P < 0.05$; $**P < 0.001$.

F184C mutation will not only affect the function of the homomeric Kv1.1 channel, but it will also alter the biophysical properties of channels composed of the human Kv1.1, Kv1.4, and Kvβ1.1 subunits.

Structural and neurophysiological speculations. The S1 segment plays a critical role in homo- and heteromultimerization of Kv1.x subunits and appears to stabilize subunit interactions (5, 41, 52). The F184 amino acid resides within the S1 segment. Here, we demonstrate that a phenylalanine-to-cysteine substitution at position 184 and Zn^{2+} slow the activation kinetics of the channel as well as the N-type inactivation kinetics and reduce the inactivating current amplitude. These results suggest that the F184C mutation and Zn^{2+} stabilize the closed-channel conformation, thus delaying channel opening. N-type inactivation results from the open channel block operated by the NH_2 termini of the Kv1.4 and Kvβ1.1 subunits (47, 69). The activation and inactivation processes of Kv channels are intimately related. Therefore, it is not surprising that a slower time course of channel opening delays the onset of "ball-and-chain" block mediated by these subunits. On the contrary, an interruption of the normal time course of channel opening by N-type inactivation could account for the apparent faster activation kinetics of WT channels that we observed on coexpression of Kvβ1.1 subunits (18). The slower time course of F184C channel activation may possibly affect the time course of inactivation. Nevertheless, the functional characterization of Kv1.4-1.1I177N, Kv1.4-1.1E325D, and Kv1.4-1.1V408A channels shows that they undergo slower inactivation kinetics (unpublished results). These latter EA1 mutations either do not change or accelerate the activation kinetics of the channel (1, 16, 31). Therefore, it appears that several EA1 mutations slow N-type inactivation, regardless of their activation kinetics. Thus we cannot exclude the possibility that the F184C mutation and Zn^{2+} alter the affinity of the receptor site for the inactivation particle by allosteric modifications of the inner vestibule. Alternatively, they could change the overall structure of the nearby T1 domain, altering the predocking site for the inactivation particle before insertion into the inner vestibule (69). A similar mechanism has been suggested by Li and co-workers (34), who proposed that the EA1 mutation V408A, at an equivalent position of the Kv1.4 channel, modulates inactivation through membrane-spanning mechanisms

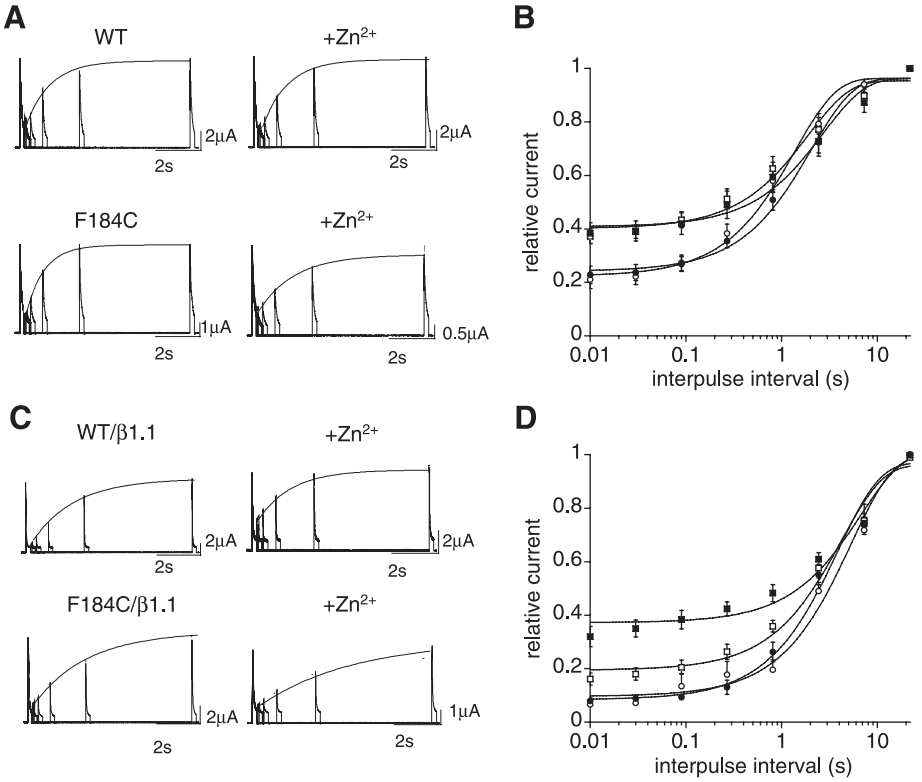

Fig. 5. Effect of Zn^{2+} on recovery from N-type inactivation. *A*: recovery from inactivation shown as representative current traces from a 2-pulse experiment. Solid lines superimposed on recovering peak current traces show fit with a single-exponential function. *B*: time course of recovery from inactivation for WT (circles) and F184C (squares) channels before (open symbols) and after (filled symbols) application of 10 μM Zn^{2+}. Current amplitude evoked by the 2nd pulse (test) was divided by that evoked by the 1st pulse (conditioning) and plotted as a function of the logarithm of the interpulse interval. Solid curves indicate fit of data points with a single-exponential function from which $\tau_{recovery}$ was calculated. *C*: time course of recovery from inactivation shown as representative current traces from a 2-pulse experiment. Solid lines superimposed on current traces show fit with a single-exponential function. *D*: relative peak currents for WT/β1.1 (circles) and F184C/β1.1 (squares) channels before (open symbols) and after (filled symbols) application of 10 μM Zn^{2+}. Relative current data points were calculated, plotted, and fitted as described in *B*. Values are means ± SE of 6–12 cells.

involving S6 (34). Nevertheless, further studies are required to assess with certainty the molecular mechanisms underlying the altered biophysical properties of the channel caused by the mutation and by Zn^{2+}.

Previous data showed that Zn^{2+} affected current amplitudes, kinetics, and voltage dependence of F184C channels also in the presence of external solutions containing higher concentrations of divalent cations such as Ca^{2+} and Mg^{2+} (14). Therefore,

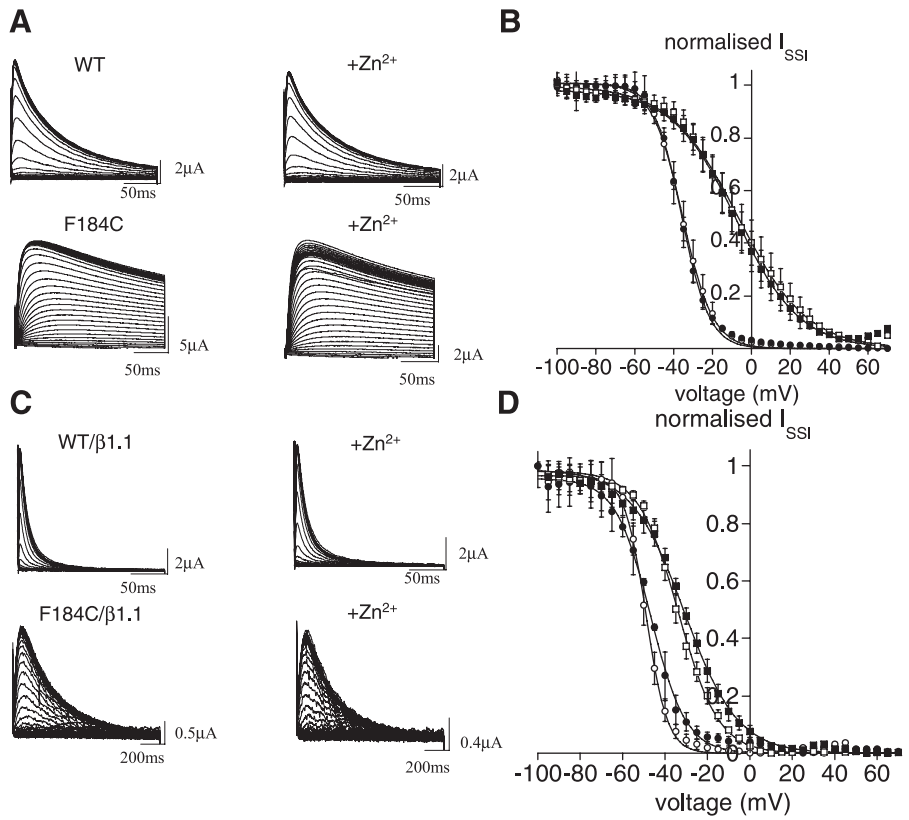

Fig. 6. Effects of F184C mutation and Zn^{2+} on voltage dependence of inactivation of heteromeric channels. *A* and *C*: sample traces recorded from oocytes before and after application of 10 μM Zn^{2+}. Currents were recorded during 100-ms depolarizing commands to +60 mV only. Traces recorded during the 1-s prepulse potentials, from −100 to +60 mV (in 5-mV increments), were omitted for clarity. *B*: voltage dependence of inactivation for WT (circles) and F184C (squares) channels calculated before (open symbols) and after (filled symbols) superfusion of 10 μM Zn^{2+}. *D*: voltage dependence of inactivation for WT/β1.1 (circles) and F184C/β1.1 (squares) channels calculated before (open symbols) and after (filled symbols) superfusion of 10 μM Zn^{2+}. Solid lines show fit of data points with a Boltzmann function. Values are means ± SE of 6–12 cells.

surface charge screening appears to be an unlikely mechanism underlying the Zn^{2+}-induced effects on F184C channels. The concentration-response relation for the Zn^{2+}-induced inhibition of the Kv1.4-1.1/Kvβ1.1 channel was well fitted with the sum of two Hill equations, suggesting the presence of two sites with which Zn^{2+} interacts. The molecular determinants of these binding sites are unknown. Recent studies of Kv1.5 channels have shown that Zn^{2+} may act on two distinct binding sites, one of which is located within the pore turret (32, 67, 68). It is possible that at least one Zn^{2+} binding site is also located within the pore turret of the Kv1.4-1.1 channel, since the amino acid sequence of this region is similar to that of the Kv1.5 channel. Unexpectedly, we also observed that the Kvβ1.1 subunits markedly decreased K_{Zn} for the low-affinity binding site. The mechanism underlying this effect is unknown. Nevertheless, allosteric modifications of the WT protein, induced by the association with the ancillary subunits, may possibly account for this phenomenon. Interestingly, the F184C mutation enhances the Zn^{2+} sensitivity of the low- and high-affinity sites. These results support the hypothesis that the F184C mutation strengthens the affinity for Zn^{2+} of sites already existing within the channel protein. Whether this occurs through allosteric changes caused by the mutation or by different mechanisms remains to be established.

The K_{Zn} values of the low- and high-affinity binding sites for Zn^{2+} on Kv1.4-1.1/Kvβ1.1 channels appear to be within the physiological range for peak Zn^{2+} concentrations at the synapse. These findings imply that Zn^{2+} may regulate the transmission of electrical signals by modulating the availability of heteromeric WT channels at synapses where Zn^{2+} is coreleased. The mossy fibers from the hippocampal CA3 area contain one of the highest concentrations of chelatable Zn^{2+} in the brain, which is assumed to be coreleased with glutamate. After release into the synaptic cleft and diffusion, hippocampal mossy fiber Zn^{2+} may modulate different pre- and postsynaptic mechanisms and may be taken up by Zn^{2+} transport systems or enter the postsynaptic neurons. Recently, it has been reported that Zn^{2+} released from mossy fibers activates presynaptic ATP-sensitive K^+ channels (6, 45). These authors concluded that the activation of such a channel type may rapidly hyperpolarize the cell, reducing Ca^{2+} influx and glutamate release. On the contrary, our results suggest that Zn^{2+} facilitates synaptic transmission by depressing the activity of presynaptic delayed-rectifier K^+ channels composed of Kv1.1, Kv1.4, and Kvβ1.1 subunits. Previous data have shown that Kv1.1, Kv1.4, and Kvβ1.1 subunits are the most likely molecular counterparts of the A-type current recorded from hippocampal mossy fiber boutons, which regulates the action potential duration and the frequency-dependent action potential broadening of the synaptic terminal (23). Here we have shown that Zn^{2+} reduces the availability of Kv1.4-1.1/Kvβ1.1 channels. These results support a model by which reduced delayed-rectifier K^+ currents broaden presynaptic action potentials during high-frequency stimuli, leading to an enhancement of intracellular Ca^{2+} signals, glutamate release, and excitatory postsynaptic potential amplitudes.

Functional properties of heteromeric channels altered by the F184C mutation and implications for EA1. Detailed biochemical studies indicate that Kv1.1, Kv1.4, and Kvβ1 subunits may also form heteromeric channels in the substantia nigra, globus pallidus, and cortical interneurons (48, 49). The results of the present study demonstrate that the F184C mutation will not only affect the function of the homomeric Kv1.1 channel, but it will also alter the biophysical properties of channels composed of the human Kv1.1, Kv1.4, and, Kvβ1.1 subunits. This evidence strongly suggests that the electrical properties of neurons within these brain structures, which coexpress these subunits, will be altered by the EA1 mutation F184C. The currents arising from the activation of Kv1.4-1.1/Kvβ1 channels possess A-type K^+ current characteristics. A-type currents regulate the firing properties of neurons, their response to input stimuli, the propagation of axonal action potential, and their backpropagation in dendrites (13, 17, 28). Because of the localization of Kv1 channel complexes on axons and terminals of hippocampal synapses, it is expected that the action potential propagation and glutamate release might be modified by the mutation (44). Precisely how will the F184C mutation affect nerve cell properties? The functional characterization of WT and F184C channels, with and without Kvβ1.1 subunits, showed that the EA1 mutation causes opposite effects on the biophysical properties of the channel. On one hand, the F184C mutation downregulates the heteromeric channel function by slowing the activation rate and increasing the time to peak current amplitude. On the other hand, this mutation increases channel availability by decreasing the rate and the amount of current undergoing N-type inactivation and by shifting the voltage dependence of inactivation in the positive direction. The relative weight of these opposite effects has yet to be determined; therefore, it is difficult to predict specifically how they will affect the electrical properties of distinct neurons.

The functional characterization of the Zn^{2+} effects on F184C channels with or without Kvβ1.1 subunits showed that this ion *1*) inhibited the F184C channels significantly more than the WT channels, *2*) further slowed the activation rate of the channel, *3*) further increased the time to reach peak current amplitude, *4*) further decreased the rate and the amount of current undergoing N-type inactivation, and *5*) slowed the repriming of the channel. First, these results demonstrate that the EA1 mutation F184C will not only sensitize the homomeric Kv1.1 channel to extracellular Zn^{2+}, but it will also endow the heteromeric channels with a higher sensitivity to Zn^{2+} when the mutated subunit is associated with the human Kv1.4 and Kvβ1.1 subunits. Although Zn^{2+} also exerts some opposite effects, it appears that this metal ion mainly depresses F184C channel functions. Therefore, it is reasonable to hypothesize that the electrical properties of mossy fibers are likely to be altered by the combined effects of the F184C mutation and Zn^{2+}. In particular, the reduced availability of Kv1.4-1.1F184C/Kvβ1.1 channels, because of their increased sensitivity to Zn^{2+}, may further increase the excitability and the frequency-dependent action potential broadening of the synaptic terminals, leading to an enhancement of intracellular Ca^{2+} signals, glutamate release, and excitatory postsynaptic potential amplitudes. Interestingly, EA1 patients report cognitive symptoms during an attack. An alteration of the transmission of the electrical signals within the hippocampus may possibly underlie this symptom (42). Moreover, epileptiform brain activity has also been associated with intracranial administration of Zn^{2+} salts, and changes in Zn^{2+} modulation of GABA receptors have been implicated in the etiology of epilepsy. Interestingly, patients bearing the F184C mutation have shown enhanced seizure susceptibility in addition to typical EA1

symptoms (60). Whether Zn^{2+} plays a role in triggering epilepsy-like symptoms in this kindred remains an intriguing hypothesis.

In conclusion, one major finding of this study is that heteromeric channels composed of the human Kv1.1 and Kv1.4 subunits have low- and high-affinity binding sites for Zn^{2+}, which are likely to regulate channel availability at distinct presynaptic membranes. We also showed that the EA1 mutation F184C alters the biophysical properties and the Zn^{2+}-induced modulation of such heteromeric channels with or without Kvβ1.1 subunits. These molecular mechanisms of EA1 are likely to exacerbate the symptoms in patients harboring the F184C mutations by altering the transmission of signals within nerve cells expressing this heteromeric channel type. Direct evidence of distinct electrical events modulated by Zn^{2+} and of overt behavioral changes caused by the F184C mutation shall be provided by the in vitro and in vivo analysis of wild-type and knock-in mice harboring such point mutation (2, 37).

ACKNOWLEDGMENTS

We thank Ezio Mezzasoma for technical assistance and Domenico Bambagioni for art work. We are grateful to the Italian Red Cross (Women's Section of Perugia) for the donation of scientific equipment to the Section of Human Physiology for this research.

Present address of A. Cusimano: Istituto di Biomedicina e Immunologia Molecolare, CNR, Via Ugo La Malfa 153, 90146 Palermo, Italy.

GRANTS

This work was financially supported by Telethon-Italy Grant GGP030159, MIUR-COFIN 2005, and Compagnia di San Paolo (Turin, Italy). P. Imbrici is the recipient of a Ph.D. fellowship from Compagnia di San Paolo.

REFERENCES

1. **Adelman JP, Bond CT, Pessia M, Maylie J.** Episodic ataxia results from voltage-dependent potassium channels with altered functions. *Neuron* 15: 1449–1454, 1995.
2. **Ashcroft MF.** *Ion Channels and Disease*. San Diego, CA: Academic, 1999.
3. **Ashizawa T, Butler IJ, Harati Y, Roongta SM.** A dominantly inherited syndrome with continuous motor neuron discharges. *Ann Neurol* 13: 285–290, 1983.
4. **Assaf SY, Chung SH.** Release of endogenous Zn^{2+} from brain tissue during activity. *Nature* 308: 734–736, 1984.
5. **Babila T, Moscucci A, Wang H, Weaver FE, Koren G.** Assembly of mammalian voltage-gated potassium channels: evidence for an important role of the first transmembrane segment. *Neuron* 12: 615–626, 1994.
6. **Bancila V, Nikonenko I, Dunant Y, Bloc A.** Zinc inhibits glutamate release via activation of pre-synaptic K channels and reduces ischaemic damage in rat hippocampus. *J Neurochem* 90: 1243–1250, 2004.
7. **Boland LM, Price DL, Jackson KA.** Episodic ataxia/myokymia mutations functionally expressed in the *Shaker* potassium channel. *Neuroscience* 91: 1557–1564, 1999.
8. **Bouchard P, Roberge C, van Gelder NM, Barbeau A.** Familial periodic ataxia responsive to acetazolamide. *Can J Neurol Sci* 11: 550–553, 1984.
9. **Bretschneider F, Wrisch A, Lehmann-Horn F, Grissmer S.** Expression in mammalian cells and electrophysiological characterization of two mutant Kv1.1 channels causing episodic ataxia type 1 (EA-1). *Eur J Neurosci* 11: 2403–2412, 1999.
10. **Browne DL, Brunt ER, Griggs RC, Nutt JG, Gancher ST, Smith EA, Litt M.** Identification of two new KCNA1 mutations in episodic ataxia/myokymia families. *Hum Mol Genet* 4: 1671–1672, 1995.
11. **Browne DL, Gancher ST, Nutt JG, Brunt ER, Smith EA, Kramer P, Litt M.** Episodic ataxia/myokymia syndrome is associated with point mutations in the human potassium channel gene, KCNA1. *Nat Genet* 8: 136–140, 1994.
12. **Brunt ER, van Weerden TW.** Familial paroxysmal kinesigenic ataxia and continuous myokymia. *Brain* 113: 1361–1382, 1990.
13. **Connor JA, Stevens CF.** Prediction of repetitive firing behaviour from voltage clamp data on an isolated neurone soma. *J Physiol* 213: 31–53, 1971.
14. **Cusimano A, D'Adamo MC, Pessia M.** An episodic ataxia type-1 mutation in the S1 segment sensitises the hKv1.1 potassium channel to extracellular Zn^{2+}. *FEBS Lett* 576: 237–244, 2004.
15. **D'Adamo MC, Imbrici P, Sponcichetti F, Pessia M.** Mutations in the KCNA1 gene associated with episodic ataxia type-1 syndrome impair heteromeric voltage-gated K^+ channel function. *FASEB J* 13: 1335–1345, 1999.
16. **D'Adamo MC, Liu Z, Adelman JP, Maylie J, Pessia M.** Episodic ataxia type-1 mutations in the hKv1.1 cytoplasmic pore region alter the gating properties of the channel. *EMBO J* 17: 1200–1207, 1998.
17. **Debanne D, Guerineau NC, Gahwiler BH, Thompson SM.** Action-potential propagation gated by an axonal I_A-like K^+ conductance in hippocampus. *Nature* 389: 286–289, 1997.
18. **De Biasi M, Wang Z, Accili E, Wible B, Fedida D.** Open channel block of human heart hKv1.5 by the β-subunit hKvβ12. *Am J Physiol Heart Circ Physiol* 272: H2932–H2941, 1997.
19. **Eunson LH, Rea R, Zuberi SM, Youroukos S, Panayiotopoulos CP, Liguori R, Avoni P, McWilliam RC, Stephenson JB, Hanna MG, Kullmann DM, Spauschus A.** Clinical, genetic, and expression studies of mutations in the potassium channel gene KCNA1 reveal new phenotypic variability. *Ann Neurol* 48: 647–656, 2000.
20. **Frederickson CJ, Koh JY, Bush AI.** The neurobiology of zinc in health and disease. *Nat Rev Neurosci* 6: 449–462, 2005.
21. **Frederickson CJ, Suh SW, Silva D, Frederickson CJ, Thompsom RB.** Importance of zinc in the central nervous system: the zinc-containing neuron. *J Nutr* 130: 1471S–1483S, 2000.
22. **Gancher ST, Nutt JG.** Autosomal dominant episodic ataxia: a heterogeneous syndrome. *Mov Disord* 1: 239–253, 1986.
23. **Geiger JR, Jonas P.** Dynamic control of presynaptic Ca^{2+} inflow by fast-inactivating K^+ channels in hippocampal mossy fiber boutons. *Neuron* 28: 927–939, 2000.
24. **Harrison NL, Radke HK, Tamkun MM, Lovinger DM.** Modulation of gating of cloned rat and human K^+ channels by micromolar Zn^{2+}. *Mol Pharmacol* 43: 482–486, 1993.
25. **Harrison NL, Gibbons SJ.** Zn^{2+}: an endogenous modulator of ligand- and voltage-gated ion channels. *Neuropharmacology* 33: 935–952, 1994.
26. **Heinemann SH, Rettig J, Graack HR, Pongs O.** Functional characterization of Kv channel β-subunits from rat brain. *J Physiol* 493: 625–633, 1996.
27. **Herson PS, Virk M, Rustay NR, Bond CT, Crabbe JC, Adelman JP, Maylie J.** A mouse model of episodic ataxia type-1. *Nat Neurosci* 6: 378–383, 2003.
28. **Hoffman DA, Magee JC, Colbert CM, Johnston D.** K^+ channel regulation of signal propagation in dendrites of hippocampal pyramidal neurons. *Nature* 387: 869–875, 1997.
29. **Horton RM, Hunt HD, Ho SN, Pullen JK, Pease LR.** Engineering hybrid genes without the use of restriction enzymes: gene splicing by overlap extension. *Gene* 77: 61–68, 1989.
30. **Howell GA, Welch MG, Frederickson CJ.** Stimulation-induced uptake and release of zinc in hippocampal slices. *Nature* 308: 736–738, 1984.
31. **Imbrici P, Cusimano A, D'Adamo MC, De Curtis A, Pessia M.** Functional characterization of an episodic ataxia type-1 mutation occurring in the S1 segment of hKv1.1 channels. *Pflügers Arch* 446: 373–379, 2003.
32. **Kehl SJ, Eduljee C, Kwan DC, Zhang S, Fedida D.** Molecular determinants of the inhibition of human Kv1.5 potassium currents by external protons and Zn^{2+}. *J Physiol* 541: 9–24, 2002.
33. **Kullmann DM, Rea R, Spauschus A, Jouvenceau A.** The inherited episodic ataxias: how well do we understand the disease mechanisms? *Neuroscientist* 7: 80–88, 2001.
34. **Li X, Bett GC, Jiang X, Bondarenko VE, Morales MJ, Rasmusson RL.** Regulation of N- and C-type inactivation of Kv1.4 by pH_o and K^+: evidence for transmembrane communication. *Am J Physiol Heart Circ Physiol* 284: H71–H80, 2003.
35. **Li Y, Hough CJ, Suh SW, Sarvey JM, Frederickson CJ.** Rapid translocation of Zn^{2+} from presynaptic terminals into postsynaptic hippocampal neurons after physiological stimulation. *J Neurophysiol* 86: 2597–2604, 2001.
36. **Litt M, Kramer P, Browne D, Gancher S, Brunt ER, Root D, Phromchotikul T, Dubay CJ, Nutt J.** A gene for episodic ataxia/myokymia maps to chromosome 12p13. *Am J Hum Genet* 55: 702–709, 1994.

37. **Long SB, Campbell EB, Mackinnon R.** Crystal Structure of a mammalian voltage-dependent *Shaker* gamily K^+ channel. *Science* 309: 897–903, 2005.
38. **Long SB, Campbell EB, Mackinnon R.** Voltage sensor of Kv1.2: structural basis of electromechanical coupling. *Science* 309: 903–908, 2005.
39. **Majumder K, De Biasi M, Wang Z, Wible BA.** Molecular cloning and functional expression of a novel potassium channel β-subunit from human atrium. *FEBS Lett* 361: 13–16, 1995.
40. **Mathie A, Sutton GL, Clarke CE, Veale EL.** Zinc and copper: pharmacological probes and endogenous modulators of neuronal excitability. *Pharmacol Ther* 111: 567–583, 2006.
41. **Mathur R, Zhou J, Babila T, Koren G.** Ile-177 and Ser-180 in the S1 segment are critically important in Kv1.1 channel function. *J Biol Chem* 274: 11487–11493, 1999.
42. **Maylie B, Bissonnette E, Virk M, Adelman JP, Maylie JG.** Episodic ataxia type 1 mutations in the human Kv1.1 potassium channel alter hKvβ1-induced N-type inactivation. *J Neurosci* 22: 4786–4793, 2002.
43. **McCormack K, McCormack T, Tanouye M, Rudy B, Stuhmer W.** Alternative splicing of the human *Shaker* K^+ channel β_1 gene and functional expression of the β_2 gene product. *FEBS Lett* 370: 32–36, 1995.
44. **Monaghan MM, Trimmer JS, Rhodes KJ.** Experimental localization of Kv1 family voltage-gated K^+ channel α- and β-subunits in rat hippocampal formation. *J Neurosci* 21: 5973–5983, 2001.
45. **Quinta-Ferreira ME, Matias CM.** Tetanically released zinc inhibits hippocampal mossy fiber calcium, zinc and synaptic responses. *Brain Res* 1047: 1–9, 2005. [Corrigenda. *Brain Res* 1063: 102–104, 2005.]
46. **Rea R, Spauschus A, Eunson L, Hanna MG, Kullmann DM.** Variable K^+ channel subunit dysfunction in inherited mutations of KCNA1. *J Physiol* 538: 5–23, 2002.
47. **Rettig J, Heinemann SH, Wunder F, Lorra C, Parcej DN, Dolly JO, Pongs O.** Inactivation properties of voltage-gated K^+ channels altered by presence of beta-subunit. *Nature* 369: 289–294, 1994.
48. **Rhodes KJ, Strassle BW, Monaghan MM, Bekele-Arcuri Z, Matos MF, Trimmer JS.** Association and colocalization of the Kvβ1 and Kvβ2 β-subunits with Kv1 α-subunits in mammalian brain K^+ channel complexes. *J Neurosci* 17: 8246–8258, 1997.
49. **Roeper J, Lorra C, Pongs O.** Frequency-dependent inactivation of mammalian A-type K^+ channel KV1.4 regulated by Ca^{2+}/calmodulin-dependent protein kinase. *J Neurosci* 15: 3379–3391, 1997.
50. **Ruppersberg JP, Schroter KH, Sakmann B, Stocker M, Sewing S, Pongs O.** Heteromultimeric channels formed by rat brain potassium-channel proteins. *Nature* 345: 535–537, 1990.
51. **Schulte U, Thumfart JO, Klocker N, Sailer CA, Bildl W, Biniossek M, Dehn D, Deller T, Eble S, Abbass K, Wangler T, Knaus HG, Fakler B.** The epilepsy-linked lgi1 protein assembles into presynaptic kv1 channels and inhibits inactivation by kvβ1. *Neuron* 49: 697–706, 2006.
52. **Shen NV, Chen X, Boyer MM, Pfaffinger PJ.** Deletion analysis of K^+ channel assembly. *Neuron* 11: 67–76, 1993.
53. **Sheng M, Tsaur ML, Jan YN, Jan LY.** Subcellular segregation of two A-type K^+ channel proteins in rat central neurons. *Neuron* 9: 271–284, 1992.
54. **Smart TG, Hosie AM, Miller PS.** Zn^{2+} ions: modulators of excitatory and inhibitory synaptic activity. *Neuroscientist* 10: 432–441, 2004.
55. **Spauschus A, Eunson L, Hanna MG, Kullmann DM.** Functional characterization of a novel mutation in KCNA1 in episodic ataxia type 1 associated with epilepsy. *Ann NY Acad Sci* 868: 442–446, 1999.
56. **Takeda A.** Movement of zinc and its functional significance in the brain. *Brain Res Brain Res Rev* 34: 137–148, 2000.
57. **Takeda A.** Zinc homeostasis and functions of zinc in the brain. *Biometals* 14: 343–351, 2001.
58. **Thompson RB, Whetsell WOJR, Maliwal BP, Fierke CA, Frederickson CJ.** Fluorescence microscopy of stimulated Zn(II) release from organotypic cultures of mammalian hippocampus using a carbonic anhydrase-based biosensor system. *J Neurosci Methods* 96: 35–45, 2000.
59. **Trimmer JS, Rhodes KJ.** Localization of voltage-gated ion channels in mammalian brain. *Annu Rev Physiol* 66: 477–519, 2004.
60. **Van Dyke DH, Griggs RC, Murphy MJ, Goldstein MN.** Hereditary myokymia and periodic ataxia. *J Neurol Sci* 25: 109–118, 1975.
61. **Vogt K, Mellor J, Tong G, Nicoll R.** The actions of synaptically released zinc at hippocampal mossy fiber synapses. *Neuron* 26: 187–196, 2000.
62. **Wang H, Kunkel DD, Schwartzkroin PA, Tempel BL.** Localization of Kv1 and Kv1.2, two K channel proteins, to synaptic terminals, somata, and dendrites in the mouse brain. *J Neurosci* 14: 4588–4599, 1994.
63. **Wang Z, Danscher G, Kim YK, Dahlstrom A, Mook JS.** Inhibitory zinc-enriched terminals in the mouse cerebellum: double-immunohistochemistry for zinc transporter 3 and glutamate decarboxylase. *Neurosci Lett* 321: 37–40, 2002.
64. **Xie XM, Smart TG.** A physiological role for endogenous zinc in rat hippocampal synaptic neurotransmission. *Nature* 349: 521–524, 1991.
65. **Zerr P, Adelman JP, Maylie J.** Episodic ataxia mutations in Kv1.1 alter potassium channel function by dominant negative effects or haploinsufficiency. *J Neurosci* 18: 2842–2848, 1998.
66. **Zerr P, Adelman JP, Maylie J.** Characterization of three episodic ataxia mutations in the human Kv1.1 potassium channel. *FEBS Lett* 43: 461–464, 1998.
67. **Zhang S, Kwan DC, Fedida D, Kehl SJ.** External K^+ relieves the block but not the gating shift caused by Zn^{2+} in human Kv1.5 potassium channels. *J Physiol* 532: 349–358, 2001.
68. **Zhang S, Kehl SJ, Fedida D.** Modulation of Kv1.5 potassium channel gating by extracellular zinc. *Biophys J* 81: 125–136, 2001.
69. **Zhou M, Morais-Cabral JH, Mann S, MacKinnon R.** Potassium channel receptor site for the inactivation gate and quaternary amine inhibitors. *Nature* 411: 657–661, 2001.
70. **Zuberi SM, Eunson LH, Spauschus A, De Silva R, Tolmie J, Wood NW, McWilliam RC, Stephenson JP, Kullmann DM, Hanna MG.** A novel mutation in the human voltage-gated potassium channel gene (Kv1.1) associates with episodic ataxia type 1 and sometimes with partial epilepsy. *Brain* 122: 817–825, 1999.